Elastic interactions between anisotropically contracting circular cells

Roman Golkov[*] and Yair Shokef[†]

*School of Mechanical Engineering and The Sackler Center for Computational Molecular and Materials Science, Tel Aviv University,
Tel Aviv 69978, Israel*

We study interactions between biological cells that apply anisotropic active mechanical forces on an elastic substrate. We model the cells as thin disks that along their perimeters apply radial, but angle-dependent forces on the substrate. We obtain analytical expressions for the elastic energy stored in the substrate as a function of the distance between the cells, the Fourier modes of applied forces, and their phase angles. We show how the relative phases of the forces applied by the cells can switch the interaction between attractive and repulsive, and relate our results to those for linear force dipoles. For long enough distances, the interaction energy decays in magnitude as a power law of the cell-cell distance with an integer exponent that generally increases with the Fourier modes of the applied forces.

I. INTRODUCTION

Mechanical forces influence the biological function at the cellular level. This is demonstrated most clearly in the experimental result that the differentiation of stem cells and their further fate depend on the mechanical properties of their environment [1–3]. There is much current research also on the effects of mechanical forces on cell division [4,5], embryonic development [6], wound healing [7], cancer metastasis [8,9], cardiac beating [10], and more. Specifically, living cells apply forces on their environment [11]. The elastic properties of this environment largely affect the forces applied by the cells [12–18], the transmission of forces through the medium [19], their projected area [20,21], and interactions between distant cells [22,23]. Cells connect to the extracellular matrix at focal adhesions, which are positioned on their surface. At these focused points cells apply on their mechanical environment contractile forces, which are roughly directed toward the center of the cell. Traction-force-microscopy experiments provide quantitative measurements showing that for cells on two-dimensional surfaces these forces are distributed along their perimeter and less in the area of contact between the cell and the substrate [24–29]. More recent experiments have measured such traction forces also in three-dimensional geometries of cells surrounded by biological gels [4,30–32]. For a review of the biological aspects of traction force generation, see [33].

In order to develop a theoretical framework, it was suggested that on a course-grained scale, the mechanical activity of each cell may be modeled as a contractile force dipole [34–36]. A *linear force dipole* is a pair of opposing point forces of the same magnitude applied at some distance one from the other [34,37,38]. Each active cell generates a deformation field in the medium around it, which is in turn felt by distant cells, leading to a mechanical interaction [39,40].

We previously studied spherically contracting cells in a three-dimensional elastic medium. We focused first on the effects of the nonlinear material properties of the medium [41,42]. We then introduced a mean-field approximation for interactions with neighboring cells [43], and subsequently considered the full geometry of deformations induced by two spherical cells [44]. For the latter case we identified an interaction mechanism that originates from shape regulation, and which does not exist for cells that do not regulate their mechanical activity due to the mechanical forces they sense [45,46]; see also [47].

Cells typically have irregular shapes and irregular internal structures, thus active traction forces are distributed in a very anisotropic manner around each cell. In this article we consider cells that adhere to the surface of an elastic substrate, and study how their anisotropic contractility influences interactions between distant cells. Actual cells have irregular shapes, and we defer the study of cell anisotropy to future work. Here, instead we limit ourselves to symmetric cells and focus on the effects of their anisotropic contractility on cell-cell interactions. Section II describes our theoretical framework for describing the anisotropic displacement field generated by circular cells on an elastic substrate, and subsequently the interaction energy between them. In Sec. III we present our results for this interaction energy for different Fourier modes of anisotropic active forces. We find that for large enough distances, the interaction energy decays algebraically with distance with an integer exponent, which generally grows with the Fourier mode. In Sec. IV we discuss our results, and specifically show how the relative phases of the Fourier modes in the two cells may cause the interaction energy to switch sign between attractive and repulsive. Section V provides concluding remarks and outlook for future work.

II. METHODS

A. Theoretical framework

We consider two *active disks* each of radius R_0 lying on the surface of a semi-infinite elastic solid with linear Hookean

[*]romango1@tau.ac.il
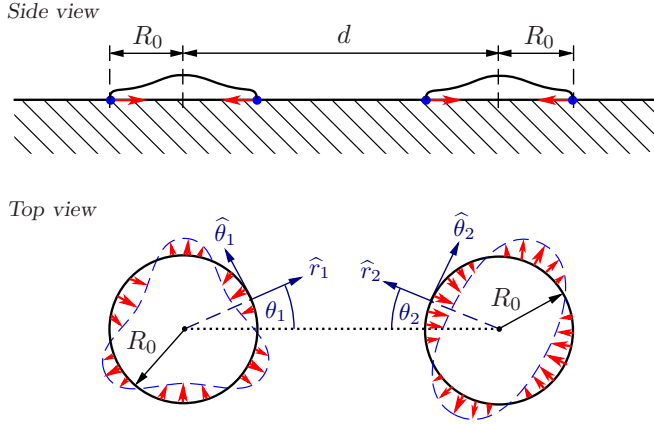[†]shokef@tau.ac.il; https://shokef.tau.ac.il/

FIG. 1. Two active disks lying on a semi-infinite medium. We use a right-handed polar coordinate system for the left disk 1 and a left-handed one for the right disk 2. Angles γ_1 and γ_2 are the phases of the Fourier components of the active forces, $f_i(\theta) = C_{n,i} \cos[n_i(\theta_i - \gamma_i)]$. In the figure $n_1 = 3$, $n_2 = 2$.

behavior defined by bulk modulus K and shear modulus G. We denote the distance between the centers of the disks by d; see Fig. 1. Each disk is adhered to the surface of the underlying material along the disk's perimeter and applies there radial active forces on the substrate in an azimuthal distribution $f(\theta)$ which is not necessarily isotropic. While the nature of such an active disk is similar to that of a linear force dipole, there are several important differences between them. First, even though cell contractility typically does not produce a propulsive force, and cell propulsion requires additional processes, here we consider also the case where the net force applied by an active disk is nonzero, namely the azimuthal distribution of active forces may include also a monopole component. Similarly, in our description, each cell's contractility may contain higher order multipole components, beyond the dipole moment that is contained in a linear force dipole.

As a result of the application of the active forces, the underlying substrate deforms and forces are transduced from one disk to the other. We shall consider the interaction energy that we define here as the difference between the work performed by two interacting active disks in the system described above and the sum of self-energies of two similar separate systems each of which includes only one such active disk. In the case we consider here of disks on a semi-infinite solid we expect the situation to be different than for three-dimensional spherical cells, in which in the absence of regulation, interaction energies vanish [44,45]. This is since for disks the displacement fields are not purely volume- or shape-changing anymore, as is the case for isotropically contracting spheres. We restrict our present analysis to the case of radial forces. One can extend our work in a straightforward manner to consider active disks that apply also azimuthal forces, and analyze that situation using a similar method to what we employ here for the case of radial forces. However, for the sake of brevity we do not include that in the present article.

Since we assume linear elastic response of the substrate, by superposition we decompose the anisotropic force distribution that each disk generates into its Fourier components, and
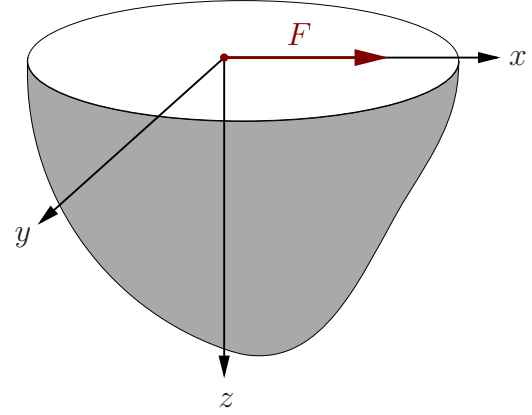

FIG. 2. Point force F on the surface of the semi-infinite medium applied in the direction of the x axis.

consider the interaction between two disks $i = 1, 2$ applying radial forces per unit length on their perimeters of the form $f_i(\theta_i) = \sum_n C_{n,i} \cos[n_i(\theta_i - \gamma_{n,i})]$; see Fig. 1. Here θ_i are the polar angles for each disk, and $\gamma_{n,i}$ are the phases of all modes. Note that live cells apply only contractile (inward) forces. However, for our mathematical analysis, which treats each mode separately, we show in Fig. 1 a single Fourier component on each disk, and those single modes have both positive and negative forces since overall each mode has to be balanced. The total force $f(\theta)$ that a cell applies is the sum of multiple such modes and is always strictly positive (inward). This is typically obtained by having a positive $n = 0$ mode.

We shall find the displacement fields created by each of the active disks and then sum them to get the total displacement, and subsequently from that we will obtain the interaction energy. We use a separate cylindrical coordinate system for each active disk with origin at its center. To simplify the calculations, we use the conventional right-handed polar coordinate system for active disk 1, on the left, while for active disk 2 on the right we will use a left-handed coordinate system; namely the angle θ_2 grows with rotation in a clockwise direction; see Fig. 1.

B. Displacement generated by active disk

To evaluate the interaction energy, we use the fact that it equals the additional work that is performed by the active disks in the presence of their neighbors. Since our active disks apply forces only on the surface of the underlying solid and since work is given by an integral of total displacement times external force at the point of application of that force, we are only interested in the displacement on the surface of the semi-infinite solid. Furthermore, to simplify our theoretical framework we limit ourselves to active forces that are purely coplanar with the free surface; see Fig. 2. Real cells on a flat substrate apply forces, which have also a component normal to the plane [48–52]. However, in this article we would like to construct a preliminary theoretical setup for understanding cell-cell interactions, thus we will limit ourselves to active disks applying only in-plane traction forces. Therefore, we will only be interested in the displacements in the same plane,

and may neglect the displacements in the direction normal to the surface.

The displacement field in the substrate must satisfy mechanical equilibrium, which we write in terms of the displacement field $\vec{u}$ as [53]

$$\frac{1}{1-2\nu}\nabla\nabla\cdot\vec{u} + \nabla^2\vec{u} = 0, \tag{1}$$

where $\nu = \frac{3K-2G}{2(3K+G)}$ is the Poisson ratio of the medium. Due to the linearity of Eq. (1) in the case of our Hookean medium, we may use the superposition principle, namely, we will decompose the angle-dependent forces created by the active disks to a system of point forces, solve the displacement field created by each of them, and finally sum the displacements to find the resultant total displacement field. We will start with the Cerrutti Green's function [54] for the displacement field due to a point force applied on the surface and in a direction tangent to the surface. Experiments often exhibit finite-depth effects, or out-of-plane traction forces [48–52]. However, for simplicity we assume the elastic medium is semi-infinite; see Fig. 2. Our theoretical framework can be extended to include also the finite thickness of the substrate, and out-of-plane active forces applied by the cells. However, we defer that to future work and limit ourselves here to the simplest case. For a force F applied at the origin and directed along the x axis (see Fig. 2), the displacement is given by [54,55]

$$u_x = \frac{F}{4\pi G}\left[\frac{1}{\rho} + \frac{x^2}{\rho^3} + (1-2\nu)\left\{\frac{1}{\rho+z} - \frac{x^2}{\rho(\rho+z)^2}\right\}\right], \tag{2}$$

$$u_y = \frac{F}{4\pi G}\left[\frac{xy}{\rho^3} - (1-2\nu)\frac{xy}{\rho(\rho+z)^2}\right], \tag{3}$$

$$u_z = \frac{F}{4\pi G}\left[\frac{xz}{\rho^3} - (1-2\nu)\frac{x}{\rho(\rho+z)}\right], \tag{4}$$

where $\rho^2 = x^2 + y^2 + z^2$. Since we are interested in plane displacements (u_x, u_y), we will ignore Eq. (4). And since we are interested in the displacements on the surface, we will set $z = 0$ in Eqs. (2) and (3). For an active disk of radius R_0 applying a radial force per unit length $f(\theta)$ along its perimeter, Eqs. (2) and (3) yield

$$du_x = f(\theta)R_0 d\theta \frac{1}{2\pi G\sqrt{x^2+y^2}}\left(1 - \nu\frac{y^2}{x^2+y^2}\right), \tag{5}$$

$$du_y = f(\theta)R_0 d\theta \frac{\nu xy}{2\pi G(x^2+y^2)^{3/2}}, \tag{6}$$

where du_x and du_y are the displacements created by the force applied along the arc $R_0 d\theta$. Here we assume that all the elastic
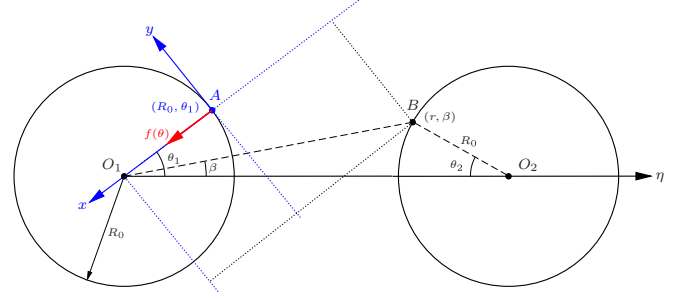

FIG. 3. Coordinate system used to evaluate the displacement at point B on the surface of active disk 2 as a result of the application of a radial point force F at point A on the boundary of active disk 1.

response is due to the substrate. That is, we ignore the elastic resistance to deformation of each cell due to the forces applied by the other cell.

In order to evaluate the displacement field created by a single active disk we first rewrite the displacement field created by a point force in cylindrical coordinates with origin at the center of that active disk. Namely, as shown in Fig. 3, we assume a force per unit length $f_1(\theta_1)$, applied at point A on the perimeter of disk 1 at orientation θ_1 with respect to $\hat{\eta}$—the axis between the centers of the disks. We then evaluate the contribution of that force to the displacement at point B, that is located on the perimeter of disk 2, namely on the surface of the medium, $z = 0$, at a distance $r = \sqrt{d^2 + R_0^2 - 2dR_0\cos\theta_2}$ from the center of disk 1, and with a polar angle $\beta = \arcsin(R_0\sin\theta_2/r)$ in disk 1. Thus for the effect of point A on the displacement at point B, we should substitute in Eqs. (2) and (3) above,

$$x = R_0 - r\cos(\theta_1 - \beta), \tag{7}$$

$$y = -r\sin(\theta_1 - \beta). \tag{8}$$

From Fig. 3 and Eqs. (7) and (8) it follows that

$$du_r = -du_x\cos(\theta_1 - \beta) - du_y\sin(\theta_1 - \beta), \tag{9}$$

$$du_\theta = -du_x\sin(\theta_1 - \beta) + du_y\cos(\theta_1 - \beta). \tag{10}$$

Here du_r and du_θ are the radial and tangential displacements of point B with respect to the origin O_1 due to the force $fR_0 d\theta$ applied by the azimuthal range $d\theta$ around point A; see Fig. 3. We substitute Eqs. (5) and (6) in Eqs. (9) and (10) and get

$$d\tilde{u}_r = -\tilde{f}(\theta_1)\frac{2(\tilde{r}^2 + 1)\cos(\theta_1 - \beta) - \tilde{r}[2 + \nu + (2-\nu)\cos(2(\theta_1 - \beta))]}{4\pi[\tilde{r}^2 - 2\tilde{r}\cos(\theta_1 - \beta) + 1]^{3/2}}d\theta_1, \tag{11}$$

$$d\tilde{u}_\theta = -\tilde{f}(\theta_1)\frac{[\tilde{r}^2(1-\nu) - \tilde{r}(2-\nu)\cos(\theta_1 - \beta) + 1]\sin(\theta_1 - \beta)}{2\pi[\tilde{r}^2 - 2\tilde{r}\cos(\theta_1 - \beta) + 1]^{3/2}}d\theta_1, \tag{12}$$

where we have defined the dimensionless displacement $\tilde{u}_r = \frac{u_r}{R_0}$, $\tilde{u}_\theta = \frac{u_\theta}{R_0}$, dimensionless force per unit length $\tilde{f}_i(\theta_i) = \frac{f_i(\theta_i)}{GR_0}$

and dimensionless position $\tilde{r} = \frac{r}{R_0}$. In order to evaluate the total displacement at point B by superposition we integrate

the contributions from all point forces $f(\theta_1)d\theta_1$ along the perimeter of active disk 1:

$$\vec{u} = \int_0^{2\pi} d\vec{u}, \tag{13}$$

with vector notation: $\vec{u} = \begin{pmatrix} \tilde{u}_r \\ \tilde{u}_\theta \end{pmatrix}, d\vec{u} = \begin{pmatrix} d\tilde{u}_r \\ d\tilde{u}_\theta \end{pmatrix}$.

C. Interaction energy

We compute the interaction energy from the additional work performed by each of the two active disks due to the presence of the neighboring active disk. To evaluate the interaction energy, we subtract from the total work the sum of the work that the same active disks would perform if there were no neighboring disks around them:

$$\Delta E = E - \sum_{i=1}^{2} E_0^{(i)}$$
$$= \frac{1}{2} \left[\sum_{i=1}^{2} \int_{L_i} (\vec{u}_{i,\text{tot}} \cdot \vec{f}_i) dL_i - \sum_{i=1}^{2} \int_{L_i} \left(\vec{u}_0^{(i)} \cdot \vec{f}_i \right) dL_i \right]$$
$$= \frac{1}{2} \sum_{i=1}^{2} \int_{L_i} \left(\left(\vec{u}_{i,\text{tot}} - \vec{u}_0^{(i)} \right) \cdot \vec{f}_i \right) dL_i, \tag{14}$$

where E is the total elastic energy stored in the medium for two interacting active disks and $E_0^{(i)}$ is the self-energy of active disk i, i.e., the elastic energy of a system that consists only of this active disk. In addition, $\vec{u}_{i,\text{tot}}$ is the total displacement at the perimeter of active disk i, $\vec{f}_i$ is the force applied by it, $\vec{u}_0^{(i)}$ is the displacement that the force $\vec{f}_i$ applied by active disk i would create in absence of the neighboring active disk, L_i is the perimeter of active disk i, and dL_i is the coordinate along it. From the last expression we see that the interaction energy is related to the product of the force applied by each disk multiplied by the displacement generated on the surface of that disk by the other disk. The coefficient $\frac{1}{2}$ in Eq. (14) may be explained in the following way [43]: Each of the active disks eventually applies some force $\vec{f}d\theta$ at each point along its edge, and the total displacement at that point is eventually $\vec{u}$. We can think of an adiabatic process during which this force was built linearly in time over a duration T such that at any time $0 < t < T$ the force is given by $\vec{g}(t)d\theta = \frac{t}{T}\vec{f}d\theta$. Then, by linearity of the medium, the displacement was built at the same rate. Namely, the displacement field at any time t is given by $\vec{\omega}(t) = \frac{t}{T}\vec{u}$. Thus the work done in this process of building the force $\vec{f}$ and the displacement $\vec{u}$ is

$$dW = \int_0^u \vec{g}(t)d\theta \, d\vec{\omega}(t)$$
$$= \frac{1}{T^2} \int_0^T t dt \cdot \vec{f}R_0 d\theta \cdot \vec{u} = \frac{1}{2}\vec{f}R_0 d\theta \cdot \vec{u}. \tag{15}$$

We now define the nondimensional interaction energy as $\Delta\tilde{E} = \frac{\Delta E}{GR_0^3}$ and rewrite Eq. (14) as

$$\Delta\tilde{E} = \frac{1}{2} \left[\sum_{i=1}^{2} \int_{2\pi} \left(\vec{\tilde{u}}_{i,\text{tot}} - \vec{\tilde{u}}_0^{(i)} \right) \cdot \vec{\tilde{f}}_i d\theta_i \right]. \tag{16}$$

Note that $\Delta\tilde{E}$ in not normalized by the self-energy E_0 but by the typical energy scale in the system, which we construct from the shear modulus of the substrate and the disk radius. According to Eq. (16) only the displacements along the perimeters of the active disks are relevant to the computation of the interaction energy. The total displacement around active disk i is

$$\vec{u}_{i,\text{tot}} = \vec{u}_i + \vec{u}_{ji} = \vec{u}_0^{(i)} + \vec{u}_{ji}. \tag{17}$$

Here $\vec{u}_i$ is the self-displacement created by disk i at its perimeter, while the displacement $\vec{u}_{ji}$ is created at the same region by the neighboring disk j. We consider the case that the forces $\vec{f}_i$ applied by the active disks do not depend on the presence of neighboring disks. Thus the self-displacement created by each active disk does not depend on the presence of neighboring disks, i.e., $\vec{u}_i = \vec{u}_0^{(i)}$. Substitution of Eq. (17) in Eq. (16) leads to [56]:

$$\Delta\tilde{E} = \frac{1}{2} \left[\sum_{i=1}^{2} \int_{2\pi} \left(\vec{\tilde{u}}_{i,\text{tot}} - \vec{\tilde{u}}_0^{(i)} \right) \vec{\tilde{f}}_i d\theta_i \right]$$
$$= \frac{1}{2} \sum_{i=1}^{2} \int_{2\pi} \vec{\tilde{u}}_{ji} \cdot \vec{\tilde{f}}_i d\theta_i$$
$$= \frac{1}{2} \left[\int_{2\pi} \vec{\tilde{u}}_{21} \cdot \vec{\tilde{f}}_1 d\theta_1 + \int_{2\pi} \vec{\tilde{u}}_{12} \cdot \vec{\tilde{f}}_2 d\theta_2 \right]. \tag{18}$$

In the general case of a system of N active disks Eq. (18) reads

$$\Delta\tilde{E} = \frac{1}{2} \sum_i \int_{2\pi} \sum_{j \neq i} \vec{\tilde{u}}_{ji} \cdot \vec{\tilde{f}}_i d\theta_i = \sum_{i \neq j} \frac{1}{2} \int_{2\pi} \vec{\tilde{u}}_{ji} \cdot \vec{\tilde{f}}_i d\theta_i. \tag{19}$$

So, an alternative way of writing the interaction energy is

$$\Delta\tilde{E} = \sum_{i \neq j} \Delta\tilde{E}_{ij}, \tag{20}$$

where

$$\Delta\tilde{E}_{ij} = \frac{1}{2} \int_{2\pi} \vec{\tilde{u}}_{ji} \cdot \vec{\tilde{f}}_i d\theta_i \tag{21}$$

is the interaction energy of active disk i with active disk j, or formulating it another way, it is the amount of additional work that active disk i performs in the presence of active disk j. Since $\vec{f}$ is in the radial direction, the product $\vec{\tilde{u}}_{ji} \cdot \vec{\tilde{f}}_i$ in Eq. (20) becomes $u_r f$ so we need only the radial part of the total displacement. However, note that we need the component of the displacement that is directed toward the center of disk i, which when analyzed in the coordinate system of disk j has both radial and azimuthal components there. It is important to emphasize that $\tilde{E}_{ij}$ and $\tilde{E}_{ji}$ have different physical meanings and are generally not necessarily equal.

The interaction energy between two active disks is $\Delta\tilde{E} = \Delta\tilde{E}_{12} + \Delta\tilde{E}_{21}$. We use Eq. (21) to compute the interaction energies $\Delta\tilde{E}_{12}$ and $\Delta\tilde{E}_{21}$. To evaluate the integral in Eq. (21) we first need to transform the displacement field generated by disk j from its coordinate system to the coordinate system of disk i. The transformation is done by multiplying the vector $d\vec{\tilde{u}}_j$, Eqs. (11) and (12) by the appropriate rotation matrix $B^{(ji)}$. Here j and i in the superscript denote the original
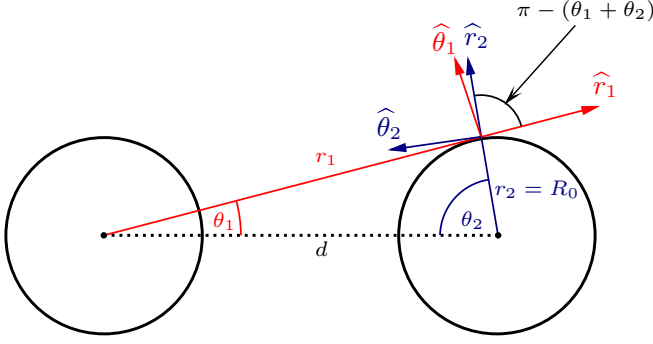
FIG. 4. Transformation of the coordinate system (r_1, θ_1) to the coordinate system (r_2, θ_2).

and the target coordinate systems, respectively. For the system depicted in Fig. 4 the rotation matrix $B^{(ji)}$ is given by

$$B^{(12)} = B^{(21)} = \begin{pmatrix} -\cos(\theta_1 + \theta_2) & \sin(\theta_1 + \theta_2) \\ \sin(\theta_1 + \theta_2) & \cos(\theta_1 + \theta_2) \end{pmatrix}, \quad (22)$$

where the first equality follows from our choice of left- and right-handed coordinate systems; see Fig. 4. The resultant displacement field is

$$\vec{u}_{12} = \begin{pmatrix} -\cos(\theta_1 + \theta_2)\tilde{u}_r + \sin(\theta_1 + \theta_2)\tilde{u}_\theta \\ \sin(\theta_1 + \theta_2)\tilde{u}_r + \cos(\theta_1 + \theta_2)\tilde{u}_\theta \end{pmatrix}. \quad (23)$$

Since the forces applied by each of the active disks are directed in the radial direction, it follows from Eq. (21) that we only need the first, radial component in Eq. (23). The interaction energy $\Delta \tilde{E}_{21}$ then becomes

$$\Delta \tilde{E}_{21} = \frac{1}{2} \int_{-\pi}^{\pi} (\vec{u}_{12} \cdot \vec{f}_2) \, d\theta_2$$

$$= \frac{1}{2} \int_{-\pi}^{\pi} [-\cos(\theta_1 + \theta_2)\tilde{u}_r$$

$$+ \sin(\theta_1 + \theta_2)\tilde{u}_\theta] \tilde{f}_2(\theta_2) d\theta_2. \quad (24)$$

As mentioned above, the interaction energy $\Delta \tilde{E}_{21}$ depends only on the radial part of the displacement $\vec{\tilde{u}}_{12}$; see Eqs. (22) and (23). The angle θ_1 in this expression originally belongs to the rotation matrix $B^{(ji)}$ [see Eqs. (22) and (23)] and will be replaced by the following expressions in terms of θ_2:

$$\tilde{r} = \sqrt{\tilde{d}^2 + 1 - 2\tilde{d} \cos \theta_2}, \quad (25)$$

$$\sin(\theta_1) = \frac{\sin \theta_2}{\tilde{r}}, \quad (26)$$

$$\cos(\theta_1) = \frac{\tilde{d} - \cos \theta_2}{\tilde{r}}, \quad (27)$$

where we have introduced the dimensionless distance between the cells $\tilde{d} = d/R_0$. In order to get $\Delta \tilde{E}_{21}$ using Eq. (24) we need to compute $\tilde{u}_r$ and $\tilde{u}_\theta$, which are the radial and tangential (with respect to O_1) components of the displacement field created by active disk 1 along the perimeter of active disk 2. We evaluate them by using trigonometric relations for $\sin(\theta - \beta)$ and $\cos(\theta - \beta)$ in Eqs. (11)–(13) and then substituting the following relations:

$$\tilde{r} = \sqrt{\tilde{d}^2 + 1 - 2\tilde{d} \cos \theta_2}, \quad (28)$$

$$\sin(\beta) = \frac{\sin \theta_2}{\tilde{r}}, \quad (29)$$

$$\cos(\beta) = \frac{\tilde{d} - \cos \theta_2}{\tilde{r}}, \quad (30)$$

which follow from the cosine theorem for the geometry of the system of two active disks, as shown in Fig. 3. See also Eqs. (25)–(27). We integrate over θ_1 in accordance with Eqs. (11)–(13) and substitute the results that do not depend on θ_1 anymore in Eq. (24) that includes instances of θ_1 that come from the rotation matrix $B^{(21)}$; see Eqs. (22)–(24). In order to complete the coordinate transformation from (r_1, θ_1) to (r_2, θ_2) we allow the same procedure that we employed for β to these remaining instances of θ_1. Namely, we substitute in Eq. (24) $\sin \theta_2/\tilde{r}$ and $(\tilde{d} - \cos \theta_2)/\tilde{r}$ for $\sin(\theta_1)$ and $\cos(\theta_1)$, respectively, in accordance with Fig. 4 and with Eqs. (25)–(27). After substitution and integration over θ_2 we evaluate the expression for $\Delta \tilde{E}_{21}$. In the same manner we evaluate $\Delta \tilde{E}_{12}$ and then in accordance with Eq. (20) we sum $\Delta \tilde{E}_{21}$ and $\Delta \tilde{E}_{21}$ to get the expression for the total interaction energy in this system.

III. RESULTS

A. Interaction between single Fourier modes

If we take $f_1(\theta_1) = A_1 \cos[n(\theta_1 - \gamma_1)]$ and $f_2(\theta_2) = A_2 \cos[m(\theta_2 - \gamma_2)]$, then from Eqs. (11) and (12) we get

$$(d\tilde{u}_r)_n = -a_1 \cos[n(\theta_1 - \gamma_1)] \frac{\{2(\tilde{r}^2 + 1)\cos(\theta_1 - \beta) - \tilde{r}[2 + \nu + (2 - \nu)\cos(2(\theta_1 - \beta))]\}}{4\pi[\tilde{r}^2 - 2\tilde{r}\cos(\theta_1 - \beta) + 1]^{3/2}} d\theta_1, \quad (31)$$

$$(d\tilde{u}_\theta)_n = -a_1 \cos[n(\theta_1 - \gamma_1)] \frac{[\tilde{r}^2(1 - \nu) - \tilde{r}(2 - \nu)\cos(\theta_1 - \beta) + 1] \sin(\theta_1 - \beta)}{2\pi[\tilde{r}^2 - 2\tilde{r}\cos(\theta_1 - \beta) + 1]^{3/2}} d\theta_1. \quad (32)$$

Here $a_i = \frac{A_i}{GR_0}$ is the dimensionless magnitude of the force, and the subscript n indicates the harmonic mode of the force. After substitution of Eqs. (28)–(30) in Eqs. (31) and (32) we get

$$(d\tilde{u}_r)_n = a_1 \cos[n(\theta_1 - \gamma_1)] \frac{\varphi}{2\kappa} d\theta_1, \quad (33)$$

$$(d\tilde{u}_\theta)_n = a_1 \cos[n(\theta_1 - \gamma_1)] \frac{\psi}{\kappa} d\theta_1, \quad (34)$$

with

$$
\begin{aligned}
\varphi \equiv {} & (2+\nu)(1+\tilde{d}^2) - 2\tilde{d}(\tilde{d}^2+3)\cos(\theta_1) \\
& + \tilde{d}^2(2-\nu)\cos(2\theta_1) + 2\tilde{d}^2\cos(\theta_1-\theta_2) \\
& - 2\tilde{d}(2+\nu)\cos(\theta_2) + 4(1+\tilde{d}^2)\cos(\theta_1+\theta_2) \\
& - 2\tilde{d}(2-\nu)\cos(2\theta_1+\theta_2) \\
& - 2\tilde{d}\cos(\theta_1+2\theta_2) + (2-\nu)\cos(2\theta_1+2\theta_2), \quad (35)
\end{aligned}
$$

$$
\begin{aligned}
\psi \equiv {} & [\tilde{d}\sin(\theta_1) - \sin(\theta_1+\theta_2)][-2-\tilde{d}^2+\nu \\
& + \tilde{d}^2\nu + \tilde{d}(2-\nu)\cos(\theta_1) + 2\tilde{d}(1-\nu)\cos(\theta_2) \\
& - (2-\nu)\cos(\theta_1+\theta_2)], \quad (36)
\end{aligned}
$$

and

$$
\begin{aligned}
\kappa \equiv {} & 2\pi\sqrt{1+\tilde{d}^2-2\tilde{d}\cos(\theta_2)}\,[2+\tilde{d}^2-2\tilde{d}\cos(\theta_1) \\
& - 2\tilde{d}\cos(\theta_2) + 2\cos(\theta_1+\theta_2)]^{3/2}. \quad (37)
\end{aligned}
$$

On substitution of these expressions in Eq. (13) and integration with respect to θ_1 we find the displacement field $\vec{\tilde{u}}_n^{(1)}$,

where the superscript 1 corresponds to the active disk that created it. In order to simplify the resultant expressions we solve for the case $\tilde{d} \gg 1$ of active disks separated by a distance which is substantially larger than their radius. Further substitution in Eq. (24) gives

$$
\begin{aligned}
\Delta\tilde{E}_{21,nm} = {} & \frac{1}{2}\int_{-\pi}^{\pi}\Big[-\cos(\theta_1+\theta_2)(\tilde{u}_r)_n^{(1)} \\
& + \sin(\theta_1+\theta_2)(\tilde{u}_\theta)_n^{(1)}\Big]\cos(m\theta_2)d\theta_2. \quad (38)
\end{aligned}
$$

Here $\Delta\tilde{E}_{21,nm}$ is the amount of additional work that active disk 2 performs due to the presence of active disk 1 if they apply radial forces $\tilde{f}_2(\theta_2) = a_2\cos[m(\theta_2-\gamma_2)]$ and $\tilde{f}_1(\theta_1) = a_1\cos[n(\theta_1-\gamma_1)]$, respectively.

B. Isotropic forces

As a demonstration of this procedure we take a simple case, in which the forces applied by the active disks are isotropic, i.e., $n = m = 0$ and thus $\tilde{f}_1(\theta_1) = \tilde{f}_2(\theta_2) \equiv 1$. In this case Eqs. (11) and (12) become

$$
d\tilde{u}_r = -\frac{\{2(\tilde{r}^2+1)\cos(\theta-\beta) - \tilde{r}[2+\nu+(2-\nu)\cos(2(\theta-\beta))]\}}{4\pi[\tilde{r}^2-2\tilde{r}\cos(\theta-\beta)+1]^{3/2}}d\theta, \quad (39)
$$

$$
d\tilde{u}_\theta = -\frac{[\tilde{r}^2(1-\nu) - \tilde{r}(2-\nu)\cos(\theta-\beta)+1]\sin(\theta-\beta)}{2\pi[\tilde{r}^2-2\tilde{r}\cos(\theta-\beta)+1]^{3/2}}d\theta. \quad (40)
$$

Here the symmetry of the applied forces results in the cancellation of u_θ, and moreover u_r does not depend on β. Thus we cancel β in Eq. (39), substitute it in Eq. (13) and get

$$
\tilde{u}_r = -\frac{(1-\nu)}{\pi\tilde{r}(1+\tilde{r})}[(1+\tilde{r}^2)K(k) - (1+\tilde{r})^2E(k)], \quad (41)
$$

which is consistent with [54]. Here $K(k)$ and $E(k)$ are the complete elliptic integrals of the first and the second kind, respectively [57]:

$$
K(x) = \int_0^{\frac{1}{2}\pi}\sqrt{1-x^2\sin^2\theta}\,d\theta, \quad (42)
$$

$$
E(x) = \int_0^{\frac{1}{2}\pi}\frac{d\theta}{\sqrt{1-x^2\sin^2\theta}}, \quad (43)
$$

and $k = \frac{2\sqrt{\tilde{r}}}{1+\tilde{r}}$. Since both active disks apply the same forces that do not depend on the phases γ_1 and γ_2, the total interaction energy equals $\Delta E = 2\Delta E_{21}$ where ΔE_{21} is given by Eq. (24). Since Eqs. (28)–(30) have to be substituted in Eq. (41), the resultant expression becomes too cumbersome to be integrated analytically in accordance with Eq. (13). For higher modes ($n, m > 0$) the equations become even more complicated and analytic solutions for the integrals in Eqs. (13) and (24) are not known. To overcome this difficulty, we approximate for large separations $\tilde{d} \gg 1$ the expressions for $d\vec{\tilde{u}}$ and $\vec{u}^{(12)}$ using a Taylor series expansion to leading order in the inverse distance $1/\tilde{d}$.

To demonstrate this in our $n = m = 0$ example, we set $a_1 = a_2 = 1$, substitute Eqs. (28)–(30) in Eqs. (39) and (40),

approximate the result to leading order in $1/\tilde{d}$ and obtain

$$
\begin{aligned}
d\tilde{u}_r = -\frac{1}{16\tilde{d}^3\pi}\big[& 4\tilde{d}(1-\nu) \\
& + (8\tilde{d}^2+5-6\nu)\cos(\theta_1) + 4\tilde{d}(1+\nu)\cos(2\theta_1) \\
& + 3(1+2\nu)\cos(3\theta_1) + 8\cos(\theta_1-2\theta_2) \\
& + 8\tilde{d}\cos(\theta_1-\theta_2) + 8(1+\nu)\cos(2\theta_1-\theta_2) \\
& + 8(1-\nu)\cos(\theta_2)\big]d\theta_1, \quad (44)
\end{aligned}
$$

$$
\begin{aligned}
d\tilde{u}_\theta = -\frac{1}{16\tilde{d}^3\pi}\big[& (8\tilde{d}^2(1-\nu)-1+3\nu)\sin(\theta_1) \\
& + 4\tilde{d}(1-2\nu)\sin(2\theta_1) + 3(1-3\nu)\sin(3\theta_1) \\
& + 8(1-\nu)\sin(\theta_1-2\theta_2) - 8\tilde{d}(1-\nu)\sin(\theta_1-\theta_2) \\
& + 8(1-2\nu)\sin(2\theta_1-\theta_2)\big]d\theta_1. \quad (45)
\end{aligned}
$$

Note that in spite of the fact that θ_2 is present in Eqs. (44) and (45), $d\tilde{u}_r$ and $d\tilde{u}_\theta$ are the radial and azimuthal displacements in the coordinate system of active disk 1. In order to rewrite them in the coordinate system of active disk 2 one has to multiply them by the rotation matrix $B^{(12)}$; see Eq. (22). We integrate Eqs. (44) and (45) according to Eq. (13) and get

$$
\tilde{u}_r = -\frac{(1-\nu)(\tilde{d}+2\cos(\theta_2))}{2\tilde{d}^3}, \quad (46)
$$

$$
\tilde{u}_\theta = 0. \quad (47)
$$

Substitution of Eqs. (46) and (47) in Eq. (23) gives the expressions for the displacement field created by active disk 1

TABLE I. Coefficients F_{nm} for computation of the interaction energy; see Eqs. (51) and (52).

$m\backslash n$	0	1	2	3	4	5	6	7	8	9
0	$\frac{1}{4}$	$\frac{1}{4}$	$\frac{3}{8}$	$\frac{15}{32}$	$\frac{35}{64}$	$\frac{315}{512}$	$\frac{693}{1024}$	$\frac{3003}{4096}$	$\frac{6435}{8192}$	$\frac{109395}{131072}$
1	$\frac{1}{4}$	$\frac{1}{4}$	$\frac{1}{8}$	$\frac{3}{32}$	$\frac{5}{64}$	$\frac{35}{512}$	$\frac{63}{1024}$	$\frac{231}{4096}$	$\frac{429}{8192}$	$\frac{6435}{131072}$
2	$\frac{3}{8}$	$\frac{1}{8}$	$\frac{1}{16}$	$\frac{3}{64}$	$\frac{5}{128}$	$\frac{35}{1024}$	$\frac{63}{2048}$	$\frac{231}{8192}$	$\frac{429}{16384}$	$\frac{6435}{262144}$
3	$\frac{15}{32}$	$\frac{3}{32}$	$\frac{3}{64}$	$\frac{9}{256}$	$\frac{15}{512}$	$\frac{105}{4096}$	$\frac{189}{8192}$	$\frac{693}{32768}$	$\frac{1287}{65536}$	$\frac{19305}{1048576}$
4	$\frac{35}{64}$	$\frac{5}{64}$	$\frac{5}{128}$	$\frac{15}{512}$	$\frac{25}{1024}$	$\frac{175}{8192}$	$\frac{315}{16384}$	$\frac{1155}{65536}$	$\frac{2145}{131072}$	$\frac{32175}{2097152}$
5	$\frac{315}{512}$	$\frac{35}{512}$	$\frac{35}{1024}$	$\frac{105}{4096}$	$\frac{175}{8192}$	$\frac{1225}{65536}$	$\frac{2205}{131072}$	$\frac{8085}{524288}$	$\frac{15015}{1048576}$	$\frac{225225}{16777216}$
6	$\frac{693}{1024}$	$\frac{63}{1024}$	$\frac{63}{2048}$	$\frac{189}{8192}$	$\frac{315}{16384}$	$\frac{2205}{131072}$	$\frac{3969}{262144}$	$\frac{14553}{1048576}$	$\frac{27027}{2097152}$	$\frac{405405}{33554432}$
7	$\frac{3003}{4096}$	$\frac{231}{4096}$	$\frac{231}{8192}$	$\frac{693}{32768}$	$\frac{1155}{65536}$	$\frac{8085}{524288}$	$\frac{14553}{1048576}$	$\frac{53361}{4194304}$	$\frac{99099}{8388608}$	$\frac{1486485}{134217728}$
8	$\frac{6435}{8192}$	$\frac{429}{8192}$	$\frac{429}{16384}$	$\frac{1287}{65536}$	$\frac{2145}{131072}$	$\frac{15015}{1048576}$	$\frac{27027}{2097152}$	$\frac{99099}{8388608}$	$\frac{184041}{16777216}$	$\frac{2760615}{268435456}$
9	$\frac{109395}{131072}$	$\frac{6435}{131072}$	$\frac{6435}{262144}$	$\frac{19305}{1048576}$	$\frac{32175}{2097152}$	$\frac{225225}{16777216}$	$\frac{405405}{33554432}$	$\frac{1486485}{134217728}$	$\frac{2760615}{268435456}$	$\frac{41409225}{4294967296}$

rewritten in the coordinate system of active disk 2. In order to evaluate the interaction energy we only need the radial component of that field:

$$(\tilde{u}_{12})_r = \frac{(1 - \nu)(\tilde{d} + 2\cos(\theta_2))(\tilde{d}\cos(\theta_2) - 1)}{2\tilde{d}^3\sqrt{\tilde{d}^2 - 2\tilde{d}\cos(\theta_2) + 1}}. \quad (48)$$

The interaction energy in accordance with Eq. (24) is

$$\Delta\tilde{E}_{21} = -\frac{\pi(1 - \nu)}{2\tilde{d}^3}. \quad (49)$$

Due to the symmetry of the system, $\Delta\tilde{E}_{12} = \Delta\tilde{E}_{21}$, thus $\Delta\tilde{E} = 2\Delta\tilde{E}_{21}$, and in dimensional form we have

$$\Delta E = -\pi(1 - \nu)GR_0^3 \frac{A_1}{GR_0} \times \frac{A_2}{GR_0}\left(\frac{R_0}{d}\right)^3. \quad (50)$$

This interaction energy clearly scales with the typical energy scale GR_0^3 in the system. It depends on the product of the dimensionless force magnitudes $a_i = \frac{A_i}{GR_0}$, and decays algebraically with the dimensionless distance $\tilde{d} = \frac{d}{R_0}$ between the disks. We get $\Delta E < 0$, which means that isotropically contracting active disks will be attracted to each other. We will later show that for higher modes, ΔE may be positive or negative depending on the phases γ_1, γ_2. Since the forces applied by the active disks in this case ($n = m = 0$) are

isotropic, the resultant interaction energy does not include γ_1 and γ_2, while for any other modes of the forces, the interaction energy will depend on them.

C. Higher modes

We find that the dimensionless interaction energies $\Delta\tilde{E}_{nm}$ between any modes n and m of the dimensionless forces $\tilde{f}_1(\theta_1) = a_1\cos[n(\theta_1 - \gamma_1)]$ and $\tilde{f}_2(\theta_2) = a_2\cos[m(\theta_2 - \gamma_2)]$ have the general form,

$$\Delta\tilde{E}_{nm} = -\frac{\pi a_1 a_2}{\tilde{d}^{|n-1|+|m-1|+1}}[(2 - \nu)F_{nm}\cos(n\gamma_1 + m\gamma_2) + \nu H_{nm}\cos(n\gamma_1 - m\gamma_2)], \quad (51)$$

where the coefficients F_{nm}, H_{nm} are given in Tables I and II for the first 10 modes. In dimensional form this is given by

$$\Delta E_{nm} = -\pi GR_0^3 \frac{A_1}{GR_0} \times \frac{A_2}{GR_0}\left(\frac{R_0}{d}\right)^{|n-1|+|m-1|+1}$$
$$\times [(2 - \nu)F_{nm}\cos(n\gamma_1 + m\gamma_2) + \nu H_{nm}\cos(n\gamma_1 - m\gamma_2)], \quad (52)$$

where $f_i(\theta_i)$ and thus A_i have dimension of force per unit length.

TABLE II. Coefficients H_{nm} for computation of the interaction energy; see Eqs. (51) and (52).

| $m\backslash n$	0	1	2	3	4	5	6	7	8	9
0	$-\frac{1}{4}$	$-\frac{1}{4}$	$-\frac{3}{8}$	$-\frac{15}{32}$	$-\frac{35}{64}$	$-\frac{315}{512}$	$-\frac{693}{1024}$	$-\frac{3003}{4096}$	$-\frac{6435}{8192}$	$-\frac{109395}{131072}$
1	$-\frac{1}{4}$	$\frac{1}{4}$	$\frac{3}{8}$	$\frac{15}{32}$	$\frac{35}{64}$	$\frac{315}{512}$	$\frac{693}{1024}$	$\frac{3003}{4096}$	$\frac{6435}{8192}$	$\frac{109395}{131072}$
2	$-\frac{3}{8}$	$\frac{3}{8}$	$\frac{15}{16}$	$\frac{105}{64}$	$\frac{315}{128}$	$\frac{3465}{1024}$	$\frac{9009}{2048}$	$\frac{45045}{8192}$	$\frac{109395}{16384}$	$\frac{2078505}{262144}$
3	$-\frac{15}{32}$	$\frac{15}{32}$	$\frac{105}{64}$	$\frac{945}{256}$	$\frac{3465}{512}$	$\frac{45045}{4096}$	$\frac{135135}{8192}$	$\frac{765765}{32768}$	$\frac{2078505}{65536}$	$\frac{43648605}{1048576}$
4	$-\frac{35}{64}$	$\frac{35}{64}$	$\frac{315}{128}$	$\frac{3465}{512}$	$\frac{15015}{1024}$	$\frac{225225}{8192}$	$\frac{765765}{16384}$	$\frac{4849845}{65536}$	$\frac{14549535}{131072}$	$\frac{334639305}{2097152}$
5	$-\frac{315}{512}$	$\frac{315}{512}$	$\frac{3465}{1024}$	$\frac{45045}{4096}$	$\frac{225225}{8192}$	$\frac{3828825}{65536}$	$\frac{14549535}{131072}$	$\frac{101846745}{524288}$	$\frac{334639305}{1048576}$	$\frac{8365982625}{16777216}$
6	$-\frac{693}{1024}$	$\frac{693}{1024}$	$\frac{9009}{2048}$	$\frac{135135}{8192}$	$\frac{765765}{16384}$	$\frac{14549535}{131072}$	$\frac{61108047}{262144}$	$\frac{468495027}{1048576}$	$\frac{1673196525}{2097152}$	$\frac{45176306175}{33554432}$
7	$-\frac{3003}{4096}$	$\frac{3003}{4096}$	$\frac{45045}{8192}$	$\frac{765765}{32768}$	$\frac{4849845}{65536}$	$\frac{101846745}{524288}$	$\frac{468495027}{1048576}$	$\frac{3904125225}{4194304}$	$\frac{15058768725}{8388608}$	$\frac{436704293025}{134217728}$
8	$-\frac{6435}{8192}$	$\frac{3003}{4096}$	$\frac{45045}{8192}$	$\frac{765765}{32768}$	$\frac{4849845}{65536}$	$\frac{101846745}{524288}$	$\frac{468495027}{1048576}$	$\frac{3904125225}{4194304}$	$\frac{15058768725}{8388608}$	$\frac{436704293025}{134217728}$
9	$-\frac{109395}{131072}$	$\frac{109395}{131072}$	$\frac{2078505}{262144}$	$\frac{43648605}{1048576}$	$\frac{334639305}{2097152}$	$\frac{8365982625}{16777216}$	$\frac{45176306175}{33554432}$	$\frac{436704293025}{134217728}$	$\frac{1933976154825}{268435456}$	$\frac{63821213109225}{4294967296}$
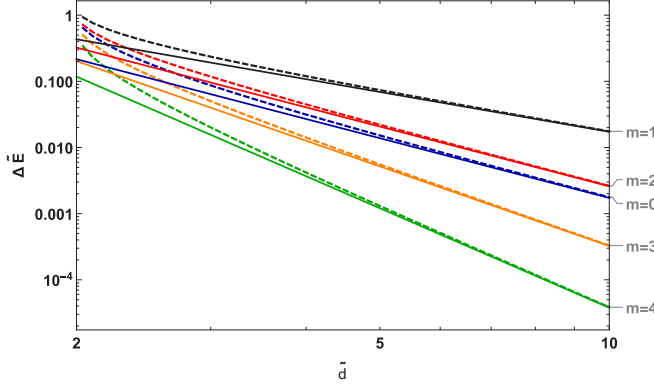
FIG. 5. Nondimensional interaction energy $\Delta \tilde{E}$ between two active disks applying radial forces $\tilde{f}_1 \equiv 1$ and $\tilde{f}_2 = \cos(m\theta_2)$ with $0 \leqslant m \leqslant 4$ vs the nondimensional distance $\tilde{d}$ between their centers. Dashed lines represent the exact numerical solution and solid lines represent the analytical approximation of Eq. (51). The value of Poisson's ratio was set to $\nu = 0.45$.

In the special case of $m = 0$ we get the following expression for the dimensionless interaction energy as a function of $\tilde{d}$ and γ_1:

$$\Delta \tilde{E}_{n0} = -\frac{a_1 a_2 \pi}{\tilde{d}^{|n-1|+2}} (1 - \nu) L_n \cos(n\gamma_1), \qquad (53)$$

with a single coefficient L_n. Similarly, when $n = 0$ we get

$$\Delta \tilde{E}_{0m} = -\frac{a_1 a_2 \pi}{\tilde{d}^{|m-1|+2}} (1 - \nu) L_m \cos(m\gamma_2). \qquad (54)$$

In order to incorporate these results in Tables I and II we set $F_{n0} = -H_{n0} = L_n/2$ and $F_{0m} = -H_{0m} = L_m/2$, and this takes care of the coefficient $(1 - \nu)$ that includes Poisson's ratio.

Figure 5 shows the normalized interaction energy $\Delta \tilde{E}$ computed numerically (exact) and analytically (approximate) vs the normalized distance $\tilde{d}$ between two active disks applying forces $\tilde{f}_1(\theta_1) = 1$ and $\tilde{f}_2(\theta_2) = \cos(m\theta_2)$ for $0 \leqslant m \leqslant 4$. The analytical expressions were computed using Eq. (51) and Tables I and II. As seen in the figure, for large $\tilde{d}$ the approximation of the interaction energy to the leading term is enough to capture the rate of the decay of interaction energy with $\tilde{d}$. As seen in Eq. (51) the interaction energy decays with distance as $\tilde{d}^{-q}$ where $q = |m - 1| + |n - 1| + 1$ is an integer number, which grows with the order of the term for $n, m > 0$. When the distance between the active disks is small, a good approximation requires additional terms, and thus the numerical solution may be more practical.

IV. DISCUSSION

A. Dependence on phase angles

The interaction between cells depends not only on the Fourier modes n or m that represent the wavelength of the anisotropy of contraction around each cell. Here we show how the interaction energy depends also on the relative phases of these undulations. This is formally given by Eq. (51), but more pictorially, in Fig. 6 we demonstrate the dependence of the interaction energy on the phase angle. Specifically, we show a pair of disks with an isotropic contractile force ($m = 0$) on disk 2, and a simple anisotropic force ($n = 3$) on disk 1. We
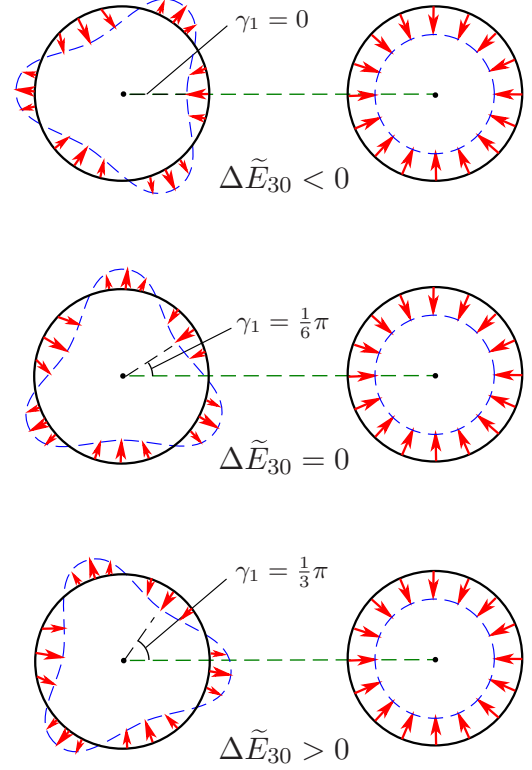

FIG. 6. System of two active disks applying forces that result in the interaction energy given by Eq. (53), demonstrating the change of sign of the interaction energy, $\Delta \tilde{E}_{30}$ as the phase angle γ_1 changes.

show different phase angles γ_1 of the force on disk 1 that give repulsive (positive), attractive (negative), and zero interaction between the disks.

As one may expect, the interaction energies are generally periodic in the phases γ_1, γ_2 since the forces are periodic; phase angles $\gamma_1 = \frac{2\pi}{n}$ and $\gamma_2 = \frac{2\pi}{m}$ are equivalent to $\gamma_1 = \gamma_2 = 0$. Indeed, all terms in Eq. (51) include the functions $\cos(n\gamma_1 \pm m\gamma_2)$. Since both functions and their derivatives are continuous and since for any $n, m > 0$, the coefficients F_{nm}, H_{nm} are positive, extremum points for any ΔE_{nm} will appear at $\{\gamma_1 = k_1 \frac{\pi}{n}, \gamma_2 = k_2 \frac{\pi}{m}\}$ with integer k_1 and k_2, where local maxima correspond to $k_1 + k_2 = 2s$ and local minima to $k_1 + k_2 = 2s + 1$ with s integer; see Fig. 7. It may also be seen that for some values of γ_1 and γ_2 the interaction energy is positive while for other values it will become negative. In other words, in some orientations the active disks will attract while in other orientations they will repel. The exact position of the $\Delta E_{nm} = 0$ lines in the (γ_1, γ_2) plane depends on the expressions for F_{nm} and H_{nm} and thus will be different for every n and m. In addition, as seen from Eq. (51) the value of Poisson's ratio ν also affects the position of the $\Delta E_{nm} = 0$ lines in the (γ_1, γ_2) plane.

B. Comparison to linear force dipoles

We mentioned earlier that we focus here on linear (Hookean) elasticity and small deformations. This allows us to use the superposition method for the force and displacements fields. Any force distribution $f_i(\theta_i)$ may be written as a
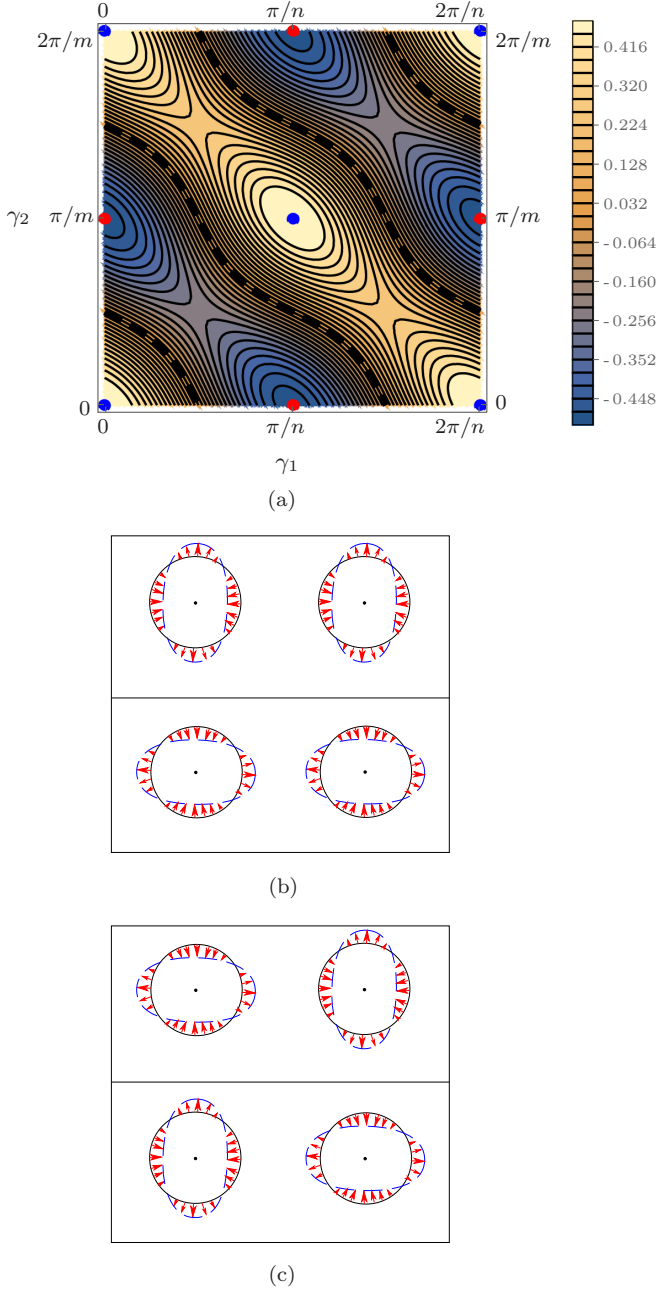
(a)

(b)

(c)

FIG. 7. (a) Typical plot of the interaction energy $\Delta\tilde{E}_{nm}$ between two anisotropic modes $n, m > 0$. Here $n = m = 1$ and $\nu = 0.45$. Thick black lines correspond to $\Delta\tilde{E}_{nm} = 0$; blue dots correspond to local maxima ($\Delta\tilde{E}_{nm} > 0$, i.e., repulsion); red dots to local minima ($\Delta\tilde{E}_{nm} < 0$, i.e., attraction). (b) and (c) Mutual orientations of active disks with $n = m = 2$ at the local maxima (b) and minima (c) of the interaction energy $\Delta\tilde{E}_{22}$.

multipole expansion using the Fourier series:

$$f_i(\theta_i) = \sum_n \{C_{n,i} \cos[n(\theta_i - \gamma_{n,i})]\}. \tag{55}$$

Mode $n = 2$ in this series is related to the linear force dipole, since it has an axis along which the forces concentrate. The interaction energy between two linear force dipoles separated by a distance d and oriented at angles γ_1 and γ_2
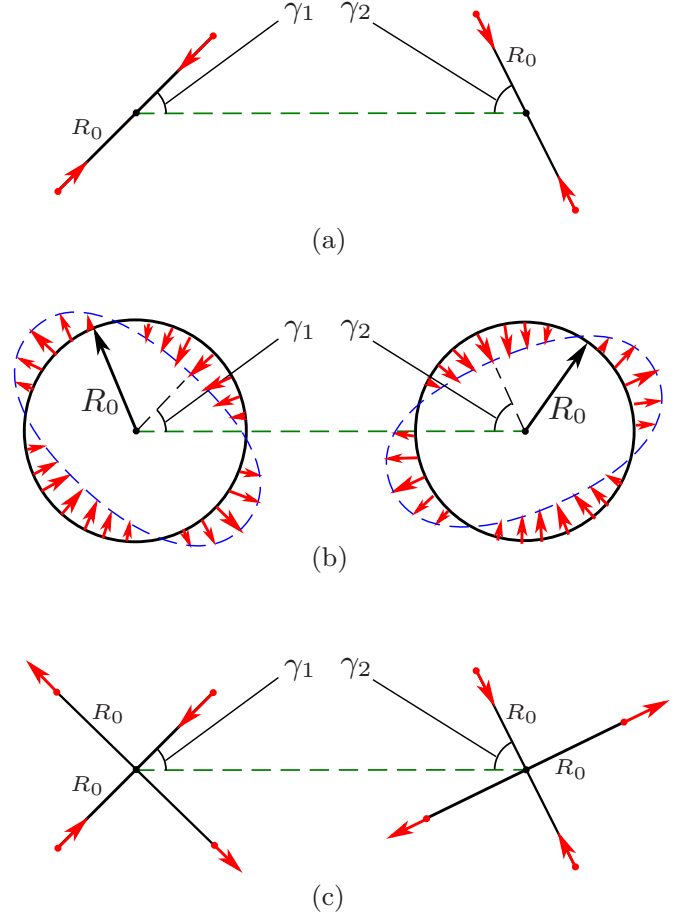

(a)

(b)

(c)

FIG. 8. Analogy of active disks to linear force dipoles. (a) Pair of linear force dipoles. (b) Pair of active disks applying mode $n = 2$ with phase angles γ_1 and γ_2. (c) Analogous system, in which each disk is replaced by two orthogonal linear force dipoles.

with respect to the axis between them [see Fig. 8(a)] is given by [40]

$$\Delta E = -\frac{F^2 R_0^2}{4\pi G d^3} \{2(1 - \nu)[1 + 3(\cos 2\gamma_1 + \cos 2\gamma_2)] \\ + 15\nu \cos(2(\gamma_1 - \gamma_2)) + (2 - \nu) \cos(2(\gamma_1 + \gamma_2))\}, \tag{56}$$

where each linear force dipole consists of two point forces F separated by a distance $2R_0$. The interaction energy we obtain from Eq. (52) for two disks applying only the $m = n = 2$ mode is

$$\Delta E = -\frac{\pi R_0^4 A_1 A_2}{16 G d^3} \{(2 - \nu) \cos[2(\gamma_1 + \gamma_2)] \\ + 15\nu \cos[2(\gamma_1 - \gamma_2)]\}. \tag{57}$$

These two expressions (56) and (57) have the same $1/d^3$ dependence on distance, but a different dependence on the relative orientations γ_1, γ_2. To make the connection between the two cases, we note that mode $n = 2$ of an active disk includes not only a concentration of two opposing contractile (inward) forces, but also a pair of extensile (outward) forces; see Fig. 8(b). Thus we compare each $n = 2$ active disk not
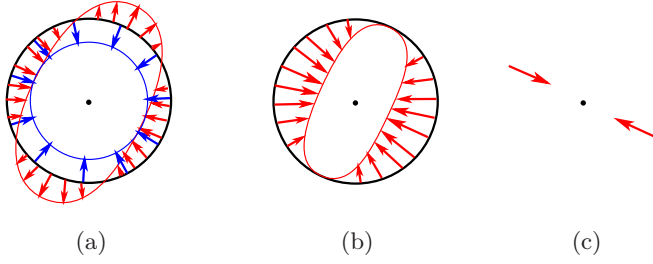
FIG. 9. Approximation of linear force dipole by superposition of $n = 0$ and $n = 2$ modes. (a) $n = 0$ (blue) and $n = 2$ (red) modes in the same coordinate system. (b) Result of the superposition of both modes. (c) The analogous linear force dipole.

to a contractile linear force dipole, but to a combination of two orthogonal linear force dipoles, one applying contraction forces and another applying expansion forces; see Fig. 8(c). We evaluated the interaction energy between two such double force dipoles using Eq. (56). We find that the angular dependence exactly matches that in the interaction between two $n = 2$ active disks as given by Eq. (57). The prefactors are matched if we set the magnitude of the force distributions to $A_1 = A_2 = \frac{4F}{\pi R_0}$.

We can also perform a comparison between our active disks and the previously studied linear force dipoles from the opposite perspective. Namely, to consider the combination of Fourier modes on a disk that best describes a linear force dipole, and compare the interaction energies obtained from each of the two models. We describe a linear force dipole by adding the isotropic mode $n = 0$ to the mode $n = 2$ on the disk in order to cancel the outward part of the radial force in the $n = 2$ mode. Namely we take $f_i(\theta_i) = A_0 + A_2 \cos[2(\theta_i - \gamma_i)]\}$; see Fig. 9. We note that in this case the spatial decay of the contributions to the interaction energy is identical for all four interaction terms (0,0), (0,2), (2,0), and (2,2), since $\Delta E \propto d^{-q}$ with $q = |n - 1| + |m - 1| + 1$. Using our far-field approximation Eq. (52), we get the following full dependence on the phase angles γ_1 and γ_2:

$$
\begin{aligned}
\Delta E &= \Delta E_{00} + \Delta E_{20} + \Delta E_{02} + \Delta E_{22} \\
&= -\frac{\pi R_0^4}{16 G d^3} \big\{ 8(1 - \nu) A_0^2 \\
&\quad + 12(1 - \nu) A_0 A_2 [\cos(2\gamma_1) + \cos(2\gamma_2)] \\
&\quad + A_2^2 [15\nu \cos(2(\gamma_1 - \gamma_2)) \\
&\quad + (2 - \nu) \cos(2(\gamma_1 + \gamma_2))] \big\}.
\end{aligned}
\tag{58}
$$

We obtain a very similar angular dependence as for the interaction between linear force dipoles. However, for this to perfectly match the expression for the interaction between two linear force dipoles (56), we would need to set $A_2 = 2A_0 = \frac{2F}{\pi R_0}$, while the geometry presented in Fig. 9 implies that $A_2 = A_0$ so that the force will vanish in the transverse direction. Nonetheless, we have established a strong connection between the previously studied model of linear force dipoles and our model of anisotropically contracting active disks.

Modes $n > 2$ can be thought of as higher-order multipoles. Mode $n = 0$ is also related to a force dipole since it is an isotropic collection of pairs of point forces around the disk.

In contrast to all other modes with zero net force, mode $n = 1$ may be thought of as a force monopole; the net force in this case does not vanish, and it is thus less relevant to nonmotile contractile cells. This is similar but not fully equivalent to electric multipoles, since in electrostatics the charges are scalar while in elasticity the forces are vectorial and thus even if we restrict ourselves to radial forces, we need to sum them vectorially in order to understand the long-range effect of these forces. Thus $n = 0$ has a meaning for forces but not for electric charges; see Refs. [41–44].

Due to the superposition principle, the dimensionless interaction energy between two active disks may be written as

$$
\Delta \tilde{E} = \sum_{n \neq m} C_{n,1} C_{m,2} \Delta \tilde{E}_{nm},
\tag{59}
$$

where the coefficients $C_{n,1}$ and $C_{m,2}$ are the amplitudes of different modes of the radial forces created by the active disks 1 and 2, respectively. From Eq. (59) it follows that knowledge of the interaction energies of different modes $\Delta \tilde{E}_{mn}$ makes it possible to evaluate the interaction energies of arbitrary force distributions $\tilde{f}_1$ and $\tilde{f}_2$.

V. CONCLUSIONS

We modeled live cells as disks resting on the surface of a semi-infinite substrate with linear (Hookean) elastic properties, and applying on the substrate, along their edges anisotropic forces directed to their centers. We described the interaction between such cells via the interaction energy, which we defined as the additional work that each cell has to perform due to the presence of the other cell. We suggest that this quantity could be helpful in theoretically predicting cellular activity. Specifically, positive interaction energy signifies repulsion or the tendency of neighboring cells to move apart or to send protrusions to opposite directions, whereas negative interaction energy would imply that cells are mechanically attracted to each other.

We found the interaction energy between every two cells to be inversely proportional to integer powers of the distance between them. This power depends on the Fourier modes, n and m of the anisotropy of the forces applied by the cells. We also found that the interaction energy is proportional to a linear combination of the functions $\cos(n\gamma_1 + m\gamma_2)$ and $\cos(n\gamma_1 - m\gamma_2)$, where γ_1 and γ_2 are the phase angles of the active forces applied by each cell. The linearity of the equations makes it possible to evaluate the interaction energy for more complex force distributions by combining the results that we presented. We deliberately simplified the biological setup to the tractable geometry of circular disks. In principle, our approach could be extended to describe cells with arbitrary shape, and not only the arbitrary azimuthal force distribution that we studied here.

Biological cells have finite thickness and finite stiffness, thus the application of forces to the substrate creates deformation fields in the cells as well and not only in the substrate, and it would be interesting to take into account the additional elastic energy stored in the cells in order to evaluate the total elastic energy of the system. Following our work on zero-thickness active disks on a semi-infinite elastic substrate,

it would be interesting to consider finite-thickness active disks with elastic properties that differ from those of the substrate. Taking into account the difference in elastic properties between the substrate and the cells will help understand the behavior of cells plated on gels with different rigidities, as tested experimentally. Finally, taking into account the nonlinearity of the substrate [13,19,41,42,58,59], our analytical procedure could clearly not be employed, and this could be an interesting direction for future numerical research.

[1] A. J. Engler, S. Sen, H. L. Sweeney, and D. E. Discher, Cell **126**, 677 (2006).

[2] J. Fu, Y-K. Wang, M. T. Yang, R. A. Desai, X. Yu, Z. Liu, and C. S. Chen, Nat. Methods **7**, 773 (2010).

[3] K. A. Kilian, B. Bugarija, B. T. Lahn, and M. Mrksich, Proc. Natl. Acad. Sci. USA **107**, 4872 (2010).

[4] A. Lesman, J. Notbohm, D. A. Tirrell, and G. Ravichandran, J. Cell Biol. **205**, 155 (2014).

[5] S. Abuhattum, A. Gefen, and D. Weihs, Integr. Biol. **7**, 1212 (2015).

[6] D. Montell, Nat. Rev. Mol. Cell Bio. **4**, 13 (2003).

[7] M. Poujade, E. Grasland-Mongrain, A. Hertzog, J. Jouanneau, P. Chavrier, B. Ladoux, A. Buguin, and P. Silberzan, Proc. Natl. Acad. Sci. USA **104**, 15988 (2007).

[8] P. Friedl and D. Gilmour, Nat. Rev. Mol. Cell Bio. **10**, 445 (2009).

[9] N. Gal and D. Weihs, Cell Biochem. Biophys. **63**, 199 (2012).

[10] I. Nitsan, S. Drori, Y. E. Lewis, S. Cohen, and S. Tzlil, Nat. Phys. **12**, 472 (2016).

[11] G. Salbreux, G. Charras, and E. Paluch, Trends Cell Biol. **22**, 536 (2012).

[12] A. Saez, A. Buguin, P. Silberzan, and B. Ladoux, Biophys. J. **89**, L52 (2005).

[13] J. P. Winer, S. Oake, and P. A. Janmey, PloS ONE **4**, e6382 (2009).

[14] M. Ghibaudo, A. Saez, L. Trichet, A. Xayaphoummine, J. Browaeys, P. Silberzan, A. Buguinb, and B. Ladoux, Soft Matter **4**, 1836 (2008).

[15] P. M. Gilbert, K. L. Havenstrite, K. E. G. Magnusson, A. Sacco, N. A. Leonardi, P. Kraft, N. K. Nguyen, S. Thrun, M. P. Lutolf, and H. M. Blau, Science **329**, 1078 (2010).

[16] O. V. Sazonova, K. L. Lee, B. C. Isenberg, C. B. Rich, M. A. Nugent, and J. Y. Wong, Biophys. J. **101**, 622 (2011).

[17] N. Nisenholz, K. Rajendran, Q. Dang, H. Chen, R. Kemkemer, R. Krishnan, and A. Zemel, Soft Matter **10**, 7234 (2014).

[18] V. B. Shenoy, H. Wang, and X. Wang, Interface Focus **6**, 20150067 (2016).

[19] R. S. Sopher, H. Tokash, S. Natan, M. Sharabi, O. Shelah, O. Tchaicheeyan, and A. Lesman, Biophys. J. **115**, 1357 (2018).

[20] B. N. Mason, A. Starchenko, R. M. Williams, L. J. Bonassar, and C. A. Reinhart-King, Acta Biomater. **9**, 4635 (2013).

[21] J. P. Califano and C. A. Reinhart-King, Cell. Mol. Bioeng. **3**, 68 (2010).

[22] C. A. Reinhart-King, M. Dembo, and D. A. Hammer, Biophys. J. **95**, 6044 (2008).

[23] Q. Shi, R. P. Ghosh, H. Engelke, C. H. Rycroft, L. Cassereau, J. A. Sethian, V. M. Weaver, and J. T. Liphardt, Proc. Natl. Acad. Sci. USA **111**, 658 (2014).

[24] M. Dembo and Y-L. Wang, Biophys. J. **76**, 2307 (1999).

[25] N. Q. Balaban, U. S. Schwarz, D. Riveline, P. Goichberg, G. Tzur, I. Sabanay, D. Mahalu, S. Safran, A. Bershadsky, L. Addadi, and B. Geiger, Nat. Cell Biol. **3**, 466 (2001).

[26] S. Munevar, Y-L. Wang, and M. Dembo, Biophys. J. **80**, 1744 (2001).

[27] K. A. Beningo, M. Dembo, I. Kaverina, J. V. Small, and Y. L. Wang, J. Cell Biol. **153**, 881 (2001).

[28] N. Wang, I. M. Tolic-Norrelykke, J. Chen, S. M. Mijailovich, J. P. Butler, J. J. Fredberg, and D. Stamenovic, Am. J. Physiol.-Cell Ph. **282**, C606 (2002).

[29] Y. Aratyn-Schaus and M. L. Gardel, Curr. Biol. **20**, 1145 (2010).

[30] W. R. Legant, J. S. Miller, B. L. Blakely, D. M. Cohen, G. M. Genin, and C. S. Chen, Nat. Methods **7**, 969 (2010).

[31] J. Notbohm, A. Lesman, D. A. Tirrell, and G. Ravichandran, Integr. Biol. **7**, 1186 (2015).

[32] J. Steinwachs, C. Metzner, K. Skodzek, N. Lang, I. Thievessen, C. Mark, S. Münster, K. E. Aifantis, and B. Fabry, Nat. Methods **13**, 171 (2016).

[33] J. T. Parsons, A. R. Horwitz, and M. A. Schwartz, Nat. Rev. Mol. Cell. Biol. **11**, 633 (2010).

[34] U. S. Schwarz and S. A. Safran, Phys. Rev. Lett. **88**, 048102 (2002).

[35] U. S. Schwarz, N. Q. Balaban, D. Riveline, A. Bershadsky, B. Geiger, and S. A. Safran, Biophys. J. **83**, 1380 (2002).

[36] U. S. Schwarz and S. A. Safran, Rev. Mod. Phys. **85**, 1327 (2013).

[37] I. B. Bischofs, S. A. Safran, and U. S. Schwarz, Phys. Rev. E **69**, 021911 (2004).

[38] I. B. Bischofs and U. S. Schwarz, Proc. Natl. Acad. Sci. USA **100**, 9274 (2003).

[39] I. B. Bischofs and U. S. Schwarz, Phys. Rev. Lett. **95**, 068102 (2005).

[40] I. B. Bischofs and U. S. Schwarz, Acta Biomater. **2**, 0510391 (2006).

[41] Y. Shokef and S. A. Safran, Phys. Rev. Lett. **108**, 178103 (2012).

[42] Y. Shokef and S. A. Safran, Phys. Rev. Lett. **109**, 169901(E) (2012).

[43] D. Ben-Yaakov, R. Golkov, Y. Shokef, and S. A. Safran, Soft Matter **11**, 1412 (2015).

[44] R. Golkov and Y. Shokef, New J. Phys. **19**, 063011 (2017).

[45] G. Sines and R. Kikuchi, Acta Metallurgica **6**, 500 (1958).

[46] T. Mura, *Micromechanics of Defects in Solids*, 2nd ed. (Kluwer Academic Publishers, Dordrecht, 1991).

[47] P. W. Oakes, S. Banerjee, M. C. Marchetti, and M. L. Gardel, Biophys. J. **107**, 825 (2014).

[48] S. A. Maskarinec, C. Franck, D. A. Tirrell, and G. Ravichandran, Proc. Natl. Acad. Sci. USA **106**, 22108 (2009).

[49] S. S. Hur, Y. Zhao, Y. S. Li, E. Botvinick, and S. Chien, Cell Mol. Bioeng. **2**, 425 (2009).

[50] A. Buxboim, K. Rajagopal, A. E. X. Brown, and D. E. Discher, J. Phys.: Condens. Matter **22**, 194116 (2010).

[51] H. Delanoë-Ayari, J. P. Rieu, and M. Sano, Phys. Rev. Lett. **105**, 248103 (2010).

[52] C. Franck, S. A. Maskarinec, D. A. Tirrell, and G. Ravichandran, PLoS ONE **6**, e17833 (2011).

[53] A. I. Lur'e, in *Three-Dimensional Problems of the Theory of Elasticity*, English ed. (Interscience Publishers, Hoboken, 1964), Chap. 6.

[54] K. L. Johnson, *Contact Mechanics*, 9th ed. (Cambridge University Press, Cambridge, 2003).

[55] S. He, Y. Su, B. Ji, and H. Gao, J. Mech. Phys. Solids **70**, 116 (2014).

[56] J. D. Eshelby, Solid State Phys. **3**, 79 (1956).

[57] http://mathworld.wolfram.com/topics/EllipticIntegrals.html.

[58] X. Xu and S. A. Safran, Phys. Rev. E **92**, 032728 (2015).

[59] X. Xu and S. A. Safran, Phys. Rev. E **95**, 052415 (2017).